1521-009X/50/9/1126–1131$35.00
DRUG METABOLISM AND DISPOSITION

dx.doi.org/10.1124/dmd.122.000902
Drug Metab Dispos 50:1126–1131, September 2022

The rs35217482 (T755I) Single-Nucleotide Polymorphism in Aldehyde Oxidase-1 Attenuates Protein Dimer Formation and Reduces the Rates of Phthalazine Metabolism[S]

Hinata Ueda, Katsuya Narumi, Ayako Furugen, Yoshitaka Saito, and Masaki Kobayashi

Laboratory of Clinical Pharmaceutics & Therapeutics, Division of Pharmasciences (H.U., K.N., A.F., M.K.) and Education Research Center for Clinical Pharmacy (K.N., M.K.), Faculty of Pharmaceutical Sciences, Hokkaido University, Sapporo, Japan; and Department of Pharmacy, Hokkaido University Hospital, Sapporo, Japan (Y.S.)

Received March 16, 2022; accepted June 23, 2022

ABSTRACT

Aldehyde oxidase-1 (AOX1) is a molybdenum-containing enzyme that catalyzes the oxidation of a range of aldehyde compounds and clinical drugs, including azathioprine and methotrexate. The purpose of this study was to elucidate the effects of single-nucleotide polymorphisms (SNPs) in the coding regions of the human *AOX1* gene on protein dimer formation and metabolic activity. Six variants [Q314R (rs58185012), I598N (rs143935618), T755I (rs35217482), A1083G (rs139092129), N1135S (rs55754655), and H1297R (rs3731722)], with allele frequencies greater than 0.01 in 1 or more population, were obtained from the genome aggregation and 1000 Genomes Project databases. Protein expression and dimer formation were evaluated using HEK293T cells expressing the wild-type (WT) or different SNP variants of AOX1. Kinetic analyses of phthalazine oxidation were performed using S9 fractions of HEK293T cells expressing WT or each the different mutant AOX1. Although we detected no significant differences among WT AOX1 and the different variants with respect to total protein expression, native PAGE analysis indicated that one of the SNP variants, T755I, found in East Asian populations, dimerizes less efficiently than the WT AOX1. Kinetic analysis, using phthalazine as a typical substrate, revealed that this mutation contributes to a reduction in the maximal rates of reaction without affecting enzyme affinity for phthalazine. Our observation thus indicates that the T755I variant has significantly negative effects on both the dimer formation and in vitro catalytic activity of AOX1. These findings may provide valuable insights into the mechanisms underlying the interindividual differences in the therapeutic efficacy or toxicity of AOX1 substrate drugs.

SIGNIFICANCE STATEMENT

The T755I (rs35217482) single-nucleotide polymorphism variant of the aldehyde oxidase-1 (AOX1) protein, which is prominent in East Asian populations, suppresses protein dimer formation, resulting in a reduction in the reaction velocity of phthalazine oxidation to less than half of that of wild-type AOX1.

Introduction

Aldehyde oxidase (AOX) is a molybdo-flavoenzyme that contributes to phase I drug metabolism. Although four AOX isoforms have been identified in mammals, only *AOX1* has been identified as an AOX functional gene in humans (Garattini et al., 2008). The AOX1 protein has a cytosolic localization, occurring primarily in the homodimeric or monomeric forms, and catalyzes the oxidation of a range of aldehydes and N-containing heterocyclic drugs, including azathioprine, famciclovir, and methotrexate (Obach et al., 2004; Kitamura et al., 2006), or the reduction of aromatic nitro-compounds, including nitrazepam and dantrolene (Konishi et al., 2017; Amano et al., 2018). The findings of several studies have indicated the clinical importance of drug-drug interactions involving AOX1 substrates or inhibitors, as exemplified in a recent case of methotrexate-induced liver toxicity following the coadministration of favipiravir (a substrate of AOX1) in a patient with osteosarcoma (Demir et al., 2022). In this respect, it is predicted that the inhibition of AOX1 would be an effective approach in preventing methotrexate metabolism and thereby enhancing its efficacy (Morgan and Baggott, 2019). Consequently, the enzyme activity of AOX1 should be taken into consideration when patients treated with AOX1 substrate drugs at standard doses exhibit abnormal clinical responses.

Large interindividual differences in the expression level and enzymatic activity of AOX1 have been observed among human liver samples. For example, Fu et al. (2013) have previously reported approximately threefold differences in the expression of AOX1 protein in samples of hepatocyte cytosols collected from 20 human patients. Additionally, a greater than 90-fold difference has been detected in the intrinsic clearance of carbazeran, a substrate of AOX1. Such interindividual differences in metabolic activity and pharmacokinetics can often be ascribed to genetic variation, and in this regard, several single-nucleotide polymorphisms (SNPs) have been reported to have an influence on AOX activity. Among these, the two SNPs N1135S (rs55754655) and H1297R (rs3731722), located in the coding regions of the *AOX1* gene, have frequently been

This work was supported in part by a Hokkaido University DX Doctoral Fellowship [grant number JPMJSP2119 to H.U.] and the Japan Society for the Promotion of Science KAKENHI [grant number JP20K07063 to K.N.].

The authors declare no conflicts of interest.

dx.doi.org/10.1124/dmd.122.000902.

[S] This article has supplemental material available at dmd.aspetjournals.org.

ABBREVIATIONS: 1KGP, 1000 Genomes Project; AOX, aldehyde oxidase; gnomAD, genome aggregation database; K_m, michaelis constant; Moco, molybdopterin cofactor; nsSNP, nonsynonymous single-nucleotide polymorphism; SNP, single-nucleotide polymorphisms; UPLC-MS/MS, ultra-performance liquid chromatography/tandem mass spectrometry; WT, wild-type; XDH, xanthine dehydrogenase.

investigated in clinical research, owing to their high allele frequencies. For example, using an *Escherichia coli* expression system, Hartmann et al. (2012) found that AOX1 harboring these SNPs is characterized by a higher catalytic efficiency with phenanthridine as a substrate. The N1135S variant has also been associated with the lack of a therapeutic effect against inflammatory bowel disease in patients receiving azathioprine (Smith et al., 2009), whereas Hutzler et al. (2014) detected an at least 17-fold difference in O^6-benzylguanine oxidation activity using cryopreserved human hepatocytes and reported that, although not significant, AOX1 harboring the two SNPs showed a tendency for higher catalytic activity. Another SNP, namely S1271L (rs141786030), found in an Italian population, is located proximate to the E1270 residue, which is essential for oxidation activity, and has been found to be associated with lower catalytic constant and michaelis constant (K_m) values compared with those of the wild-type (WT) enzyme (Foti et al., 2016). In addition to these SNPs, certain nonsynonymous SNPs (nsSNPs) are assumed to induce protein structural labialization, based on the findings of an in silico analysis (Coelho et al., 2019). Collectively, the findings of the aforementioned studies indicate that AOX1 can play a potentially important role in interindividual drug responses, and consequently, it is of particular importance that we gain an understanding of the molecular mechanisms underlying the interindividual variability of this enzyme's activity.

The goal of this study was to identify SNP variants associated with differences in human AOX1 function. To this end, we focused on the common nsSNPs found in some genome variation databases representing different races. We identified six AOX1 mutations [Q314R (rs58185012), I598N (rs143935618), T755I (rs35217482), A1083G (rs139092129), N1135S (rs55754655), and H1297R (rs3731722)] and evaluated the oxidative activity of the respective variants against phthalazine, a common substrate of AOX1. Among these six variants, AOX1 harboring the T755I (rs35217482) SNP was found to be characterized by a less efficient dimerization compared with that of the WT protein and exhibited lower catalytic activity with respect to the oxidation of phthalazine.

Materials and Methods

Chemicals. Phthalazine was purchased from Sigma-Aldrich Chemical Corp. (St. Louis, MO), phthalazone was obtained from Tokyo Chemical Industry Co. (Tokyo, Japan), and carbamazepine was from FUJIFILM Wako Pure Chemical Corp. (Osaka, Japan). All other chemicals and reagents were of commercial origin and the highest grade available.

nsSNP Retrieval and Prediction of Protein Stability. nsSNPs of the *AOX1* gene were identified based on searches of the 1000 Genome Project (1KGP) (Auton et al., 2015) and genome aggregation (gnomAD) (Karczewski et al., 2020) databases. We specifically selected all common variants: 1) minor allele frequency greater than 1% in each race and 2) located in the coding region.

Cloning of AOX1 Variants. The coding sequence (cDNA published in NM_001159) of human WT AOX1 was custom synthesized by Eurofins Genomics (Tokyo, Japan). The synthetic gene was subcloned into the NotI and XhoI sites of a pcDNA3.1(+) vector (Invitrogen, Carlsbad, CA). AOX1 variants (Q314R, I598N, T755I, A1083G, N1135S, and H1297R) were generated using a QuikChange II Site-Directed Mutagenesis Kit (Agilent Technologies, Santa Clara, CA). The sequences of the primers used for synthesis are listed in Supplemental Table 1. All constructs were confirmed by dye-terminator sequencing techniques using a BigDye Terminator v3.1 Cycle Sequencing Kit (Thermo Fisher Scientific, Waltham, MA), the results of which are shown in Supplemental Fig. 1.

Cell Culture and Transfection. Cells of the HEK293T line used in this study were cultured in Dulbecco's modified Eagle's medium supplemented with 10% fetal bovine serum and incubated at 37°C in a 5% CO_2 atmosphere. For the expression of AOX1, the cells were transiently transfected with WT or variant AOX1 plasmids using Lipofectamine 3000 (Invitrogen) at 24 hours after seeding. Cells were harvested after 48 hour of transfection and suspended in water for western blot analysis or in 0.1 M potassium phosphate buffer (pH 7.4) for evaluation of AOX1 enzymatic activity. Cell suspensions were disrupted by sonication and centrifuged at 9000*g* for 20 minutes at 4°C to obtain S9 fractions.

Visualization of nsSNPs in the Crystal Structure. A crystal structure of AOX1 was obtained from among the crystal structures of human AOX1 (Protein Data Bank: 4UHW) (Coelho et al., 2015). The locations of the targeted amino acids and small molecules are shown by stick representation, and macromolecules are depicted by either a cartoon or surface representation using PyMOL.

SDS- andNative-PAGE/Western Blot Analysis. The expression and quantities of AOX1 homodimers or monomers were evaluated by SDS- or native-PAGE western blot analysis. The S9 fractions obtained from AOX1-expressing cells were mixed with an equal volume of 2× SDS sample buffer [0.1 M Tris-HCl (pH 6.8), 4% SDS, 10% 2-mercaptoethanol, 20% glycerol, and 0.004% bromophenol blue] for SDS-PAGE or 2× sample buffer [0.1 M Tris-HCl (pH 6.8), 20% glycerol, and 0.004% bromophenol blue] for native-PAGE. SDS-PAGE was performed using 10% polyacrylamide gels containing SDS, and native-PAGE using 8%–25% gradient polyacrylamide gels. For both analyses, proteins were transferred electrophoretically to polyvinylidene difluoride membranes at 15 V for 90 minutes in transfer buffer (48 mM Tris, 39 mM glycine, 0.13 mM SDS, and 20% MeOH). The membranes were blocked with 1% nonfat dry milk in phosphate-buffered saline containing 0.05% Tween 20 and incubated overnight with a rabbit AOX1-specific primary antibody (19495-1-AP; Proteintech Group Inc., Rosemont, IL) at a 1:1000 dilution or a rabbit monoclonal anti-actin antibody (ab179467; abcam, Cambridge, UK) at a 1:5000 dilution. Having been washed with phosphate-buffered saline containing 0.05% Tween 20, the membranes were incubated with mouse anti-rabbit IgG–horseradish peroxidase secondary antibody (Santa Cruz Biotechnology, Dallas, TX) (diluted 1:4000). Bands on the membrane were detected using enhanced chemiluminescence according to the manufacturer's instructions (GE Healthcare Life Sciences) and quantified using ImageJ software.

Enzyme Assays. S9 fractions obtained from HEK293T cells in 0.1 M potassium phosphate buffer (pH 7.4) were incubated for 3 minutes at 37°C (at final concentrations of 1 to 1.4 mg protein per mL). Reactions were initiated by addition of the AOX1 substrate phthalazine in dimethyl sulfoxide (final concentration of less than 0.1%) to the prewarmed S9 fractions. The volume of the total reaction mixture was 50 μL. Following incubation, reactions were terminated by the addition of methanol containing an internal standard (carbamazepine), and the samples were then centrifuged at 16,000*g* for 15 minutes at 4°C. The supernatants thus obtained were used for analysis for the metabolite phthalazone using ultra-performance liquid chromatography/tandem mass spectrometry (UPLC-MS/MS), as described in the following section.

UPLC-MS/MS Analysis. UPLC-MS/MS analysis was conducted following the procedures described by Obach et al. (2004). The concentration of phthalazone was monitored using a Waters ACQUITY UPLC H-Class System coupled with a Xevo TQ-S mass spectrometer (Milford, MA). Individual samples (10 μL) were injected into a Waters ACQUITY UPLC BEH C18 column (1.7 μm, 2.1 × 50 mm) at 40°C and a flow rate of 0.4 mL/min. The mobile phase consisted of methanol (mobile phase A) and 0.1% formic acid in water (mobile phase B). The composition of the mobile phase was altered along a linear gradient as follows: 0%–70% A for 2.5 minutes, 70% A from 2.5 to 4 minutes, and 70%–0% A from 4 to 4.1 minutes, at which it was held to 6 minutes. Mass spectrometry analysis was conducted in positive interface electrospray ionization mode using a Xevo TQ-S triple quadrupole mass spectrometer (Waters). Phthalazone and carbamazepine were detected using a multiple-reaction monitoring mode by recording m/z values from 147 to 118 and 237 to 194, respectively.

Curve Fitting and Statistical Analysis. The concentrations of substrates and volumes of produced metabolites were plotted and analyzed using SigmaPlot 14.5 (Systat Software Inc., San Jose, CA). Kinetic parameters were determined based on nonlinear regression analysis using the Michaelis-Menten kinetic model. Statistical analyses of data were performed using an unpaired Student's *t* test or one-way ANOVA followed by Dunnett's test and Tukey's post hoc test. A *P* value of less than 0.05 was taken to be indicative of a statistical significance.

Results

Allele Frequency and Pathogenesis of nsSNPs in the *AOX1* Gene. The AOX1 protein comprises 1338 amino acids grouped within three different domains: [2Fe-2S] enclosed domain I (20 kDa), FAD domain II (40 kDa), and C-terminal domain III (90 kDa) containing a molybdopterin cofactor (Moco) (Garattini et al., 2003). On the basis of our searches of the 1KGP and gnomAD databases, we identified six common nsSNPs of the *AOX1* gene distributed among different races (Table 1), which, with the exception of Q314R (rs58185012) located in domain II, were all detected in domain III. Among these, the N1135S (rs55754655) and H1297R (rs37317222) mutations were frequently detected in all assessed races, whereas I598N (rs143935618) was found in two or more races, with the exception of European and South Asian populations. Q314R and A1083G (rs139092129) were found in only African and American populations, and T755I (rs35217482) was detected only in East Asian populations.

Evaluation of Monomeric or Dimeric Expression of AOX1. To determine the levels of WT or mutated AOX1 protein expression in S9 fractions of transiently expressing HEK293T cells, we performed SDS-PAGE and western blotting analyses. Compared with the mock-treated cells, the levels of WT AOX1 protein expression were elevated (Fig. 1A), and compared with the WT protein, we detected no significant differences among the six variants (Fig. 1B). It has been established that AOX1 activity is associated with the expression of the dimeric form of this protein (Itoh et al., 2007), and thus, we further conducted native-PAGE analysis to determine ratio of dimeric to monomeric expression (Fig. 2). We accordingly observed that, compared with the WT protein, abundance of the 300 kDa dimeric form of the T755I variant was significantly downregulated by almost 30%, whereas in contrast, little or no difference was detected with respect to the other variants.

Time Course and Inhibition Assay of WT AOX1 Activity. To analyze the time-dependent enzymatic activity of AOX1, we measured the time course of WT AOX1 oxidation activity using phthalazine, a specific and highly reactive substrate of this enzyme (Panoutsopoulos and Beedham, 2004). Mixtures of phthalazine and cell lysate were incubated for different lengths of time from 1 to 30 minutes, and we accordingly detected a linear increase in amounts of the oxidative metabolite phthalazone until 15 minutes in the S9 fraction of HEK293T cells expressing AOX1 WT, although not in that of the mock cells (Fig. 3A). Obach et al. (2004) have reported the pronounced inhibition of AOX1 activity by raloxifene (IC_{50} = 2.9 nM), and thus, we investigated the inhibitory effect of raloxifene on the oxidation of phthalazine by AOX1. Irrespective of the initial phthalazine concentration, we found that the amounts of phthalazone produced were reduced by raloxifene (Fig. 3B).

Phthalazine Oxidation by WT and Variant AOX1. Next, we evaluated differences in the enzymatic activities of WT AOX1 and the six variants (Fig. 4). We detected a significant downregulation in the activity of the T755I variant compared with that of the WT enzyme. Lower reaction velocities were also recorded for each of the other five variants, although in all cases, the reduction in activity was found to be nonsignificant. These observations would thus tend to imply that the T755I mutation either alters the substrate affinity of the enzyme or modifies its oxidation activity. To calculate the saturation kinetic parameters, we measured the concentration-dependent oxidation of phthalazine and fitted the values obtained to the Michaelis-Menten kinetic model. For WT AOX1, we obtained K_m and V_{max} values of 2.28 ± 0.24 μM and 13.03 ± 4.08 nmol·min^{-1}·mg protein^{-1}, respectively, whereas the reaction rate of T755I was found to be approximately one-fourth that of WT AOX1 (V_{max} = 3.08 ± 1.40 nmol·min^{-1}·mg protein^{-1}) (Fig. 5). Similarly, the K_m value (1.09 ± 1.14 μM) calculated for this variant was lower than that of the WT, although the difference was statistically nonsignificant.

Discussion

In this study, one of the six candidate SNPs, selected based on searches of the 1KGP and gnomAD databases, was shown to be associated with negative effects with respect to both the dimer formation and in vitro catalytic activity of AOX1. To the best of our knowledge, this is the first study to establish an association between AOX1 T755I (rs35217482) and a lower activity of human AOX1.

Our initial selection of candidate SNPs (i.e., Q314R, I598N, T755I, A1083G, N1135S, and H1297R) was based on the following two criteria: 1) SNPs with a minor allele frequency greater than 1% and 2) SNPs located within the coding regions of the human *AOX1* gene. With the exception of T755I, we detected no significant changes in the levels of total protein expression or dimer formation in the remaining five AOX1

TABLE 1

Minor allele frequency of nonsynonymous mutation in the *AOX1* gene

Data were obtained from the 1KGP and gnomAD databases. The sample size of each race is denoted in parentheses.

1KGP

		Population (n)				
NCBI SNP ID	Aino Acid Change	African (1322)	American (694)	Europe (1006)	East Asian (1008)	South Asian (978)
rs58185012	Q314R	0.027	0.001	0	0	0
rs143935618	I598N	0.002	0.042	0	0.012	0
rs35217482	T755I	0	0	0	0.010	0
rs139092129	A1083G	0.011	0.003	0	0	0
rs55754655	N1135S	0.268	0.072	0.121	0.003	0.021
rs3731722	H1297R	0.039	0.157	0.071	0.094	0.098

gnomAD

		Population (n)								
NCBI SNP ID	Amino Acid Change	African American (8128)	Latino/ Admixed American (17,296)	Ashkenazi Jewish (5040)	European (Finnish) (19,824)	European (non-Finnish) (56,885)	East Asian (9197)	South Asian (15,308)	Other (3070)	Overall (125,748)
rs58185012	Q314R	0.023	0.001	0	0	0	0	0	0	0.002
rs143935618	I598N	0	0.065	0	0	0	0.012	0	0.007	0.010
rs35217482	T755I	0	0	0	0	0	0.012	0	0	0.001
rs139092129	A1083G	0.009	0.001	0	0	0	0	0	0	0.001
rs55754655	N1135S	0.255	0.070	0.093	0.092	0.138	0.003	0.043	0.129	0.109
rs3731722	H1297R	0.041	0.131	0.036	0.110	0.065	0.080	0.091	0.065	0.079

NCBI, National Center for Biotechnology Information.

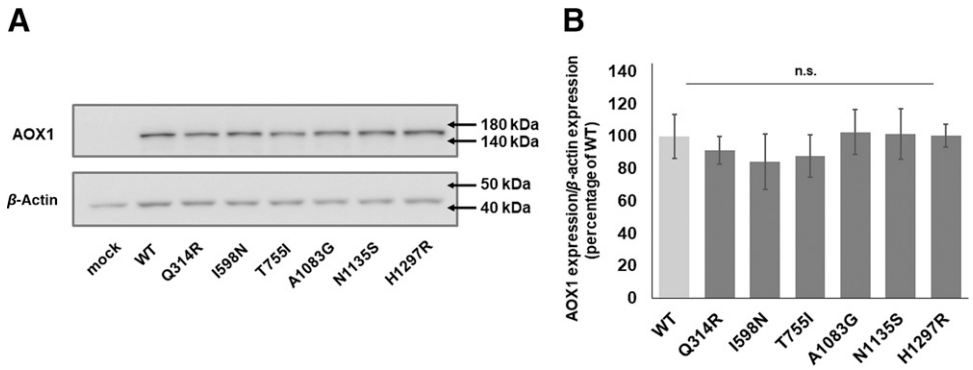

Fig. 1. The expression of WT and variant AOX1. (A) The expression of total AOX1 or β-actin protein was determined by SDS-PAGE/western blot assays. S9 fractions containing 10 μg protein were applied. (B) AOX1 protein expression was quantified and normalized relative to that of β-actin. Data are the means plus or minus S.D. of three independent experiments. n.s., not significant (Dunnett's test).

variants compared with those of the WT. Consistently, compared with the WT AOX1, we found little differences in the phthalazine oxidation activities of these five SNP variants, and thus, it can be assumed that the catalytic efficiency of AOX1 is unlikely to be affected by these mutations. Notably, Hartmann et al. (2012) have previously reported that two of the candidate SNPs, namely N1135S and H1297R, examined in the present study, were characterized by higher catalytic activities for phenanthridine compared with the WT. However, consistent with our observations, these authors detected no significant changes in the catalytic activities toward phthalazine. Similarly, Hutzler et al. (2014) reported no significant differences in the enzymic activities of these two SNP variants, although they did note a tendency for a higher catalytic activity for O^6-benzylguanine using cryopreserved human hepatocytes. In addition, the findings of several studies have indicated that N1135S is a potentially clinically relevant mutation with respect to azathioprine therapy. Accordingly, although the evidence accumulated to date indicates that the effects of AOX1 SNPs on this enzyme's catalytic activity may depend on the substrate, further prospective studies in human populations are required to confirm whether these SNPs are clinically significant.

A notable finding of the present study is the suppression of dimer formation in the T755I mutant in the absence of any marked changes in protein expression. Furthermore, this mutant is associated with a reduction in the maximal rates of reaction without affecting enzyme affinity for the substrate phthalazine. Although from the perspective of clinical significance, our findings regarding this mutant are limited to a large extent, given that we evaluated the activity of each SNP variant only with respect to phthalazine as a substrate. Our findings do, nevertheless, indicate the lower catalytic activity of the AOX1 variants compared with that of the WT AOX1. The T755 site is found to be highly conserved in a number of AOX1-like enzymes, such as mouse Aox1 (T750), mouse Aox2 (T761), mouse Aox3 (T751), mouse Aox4 (T753), rabbit Aox1 (T751), monkey Aox1 (T755), and human xanthine dehydrogenase (XDH) (T747), which show approximately 40% amino acid identity with human AOX1 (Supplemental Fig. 2). Thus, the data imply that this residue plays a pivotal role in the activity of AOX1. Further, the reduced catalytic activity of the AOX1 T755 mutant is associated with the loss of dimerization that does not entail a change in the configuration of the substrate-binding pocket. In this context, it has previously been established that the two subunits of XDH function cooperatively with respect to both the binding and catalysis of substrates (Tai and Hwang, 2004). Moreover, it has been reported that in the bacterium *Rhodobacter capsulatus*, the dimeric form of XDH comprising two [2Fe-2S] clusters is essential for Moco insertion and metabolic activation (Schumann et al., 2008). In

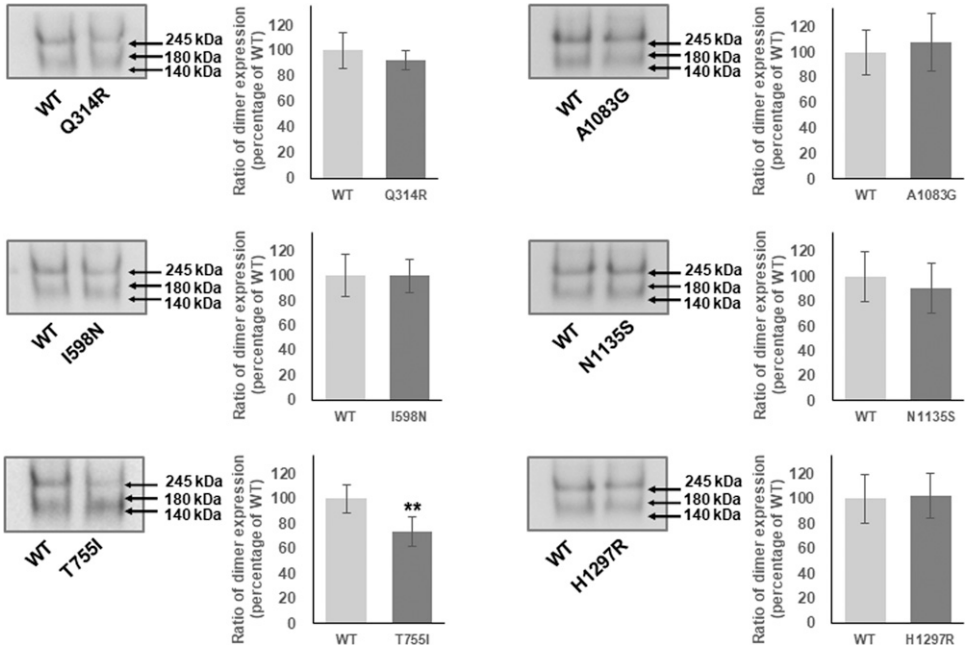

Fig. 2. Dimeric or monomeric forms of WT and variant AOX1. Dimeric or monomeric forms of AOX1 were separated by native-PAGE/western blot assays. The columns show amounts of the dimeric form of AOX1 compared with that of the WT. Dimer expression was calculated based the ratio of the area of the upper band (300 kDa) and total area of the upper and lower (150 kDa) bands. $^{**}P < 0.01$ compared with WT; unpaired Student's t test. Data are the means plus or minus S.D. of three independent experiments.

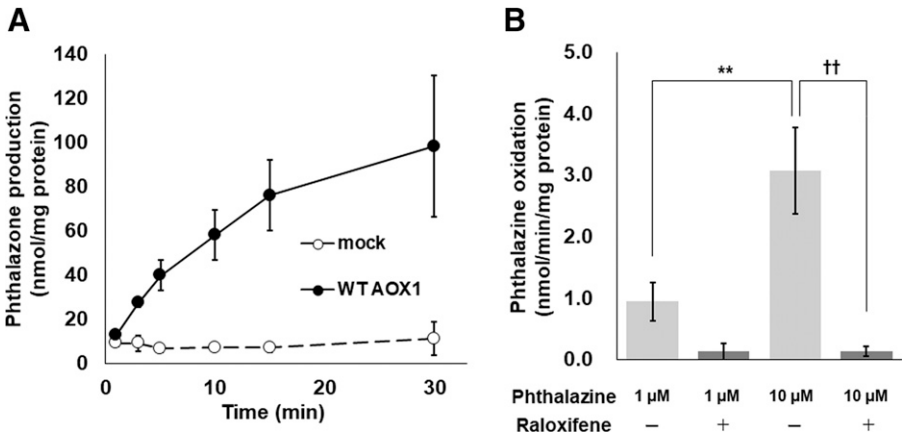

Fig. 3. Enzymatic analysis using S9 fractions of WT AOX1-overexpressing HEK293T cells. (A) Time course of phthalazine oxidation. The substrates were incubated for 1–30 minutes at a concentration of 10 μM. (B) Inhibition analysis of phthalazine metabolism. Raloxifene, a potent AOX1 inhibitor, was used at a concentration of 0.1 μM. Phthalazine (1 μM or 10 μM) was incubated for 10 minutes at pH 7.4. $^{**}P < 0.01$ compared with the 1 μM phthalazine control; $^{††}P < 0.01$ compared with the 10 μM phthalazine control; Tukey's post hoc test. Data are the means plus or minus S.D. of three independent experiments.

contrast, our current understanding regarding the mechanisms underlying the homodimerization of AOX1 is currently limited. Itoh et al. (2007) have, nevertheless, demonstrated that a G110S mutation close to the [2Fe-2S] cluster is associated with a lower degree of dimerization and a poor metabolic activity of AOX1 in Donryu rats. The amino acid G111 in human AOX1, aligned with G110 in rats, was calculated to be at about 7.7–18.8 Å from the two [2Fe-2S] clusters (Supplemental Fig. 3). Similarly, Hartmann et al. (2012) established that an R802C mutation in the vicinity of the [2Fe-2S] cluster (11.5–19.6 Å) induces the loss of dimerization in human AOX1 expressed in *E. coli*. In the present study, we also found T755 to be located close to the dimerization domain and the [2Fe-2S] cluster (Fig. 6). The distance between the T755 and [2Fe-2S] clusters was found to be 11.2–11.7 Å, similar to that of G110 and R802. Meanwhile, the N1135S SNP, located far from [2Fe-2S] clusters (~40 Å), does not change the monomer/dimer ratio compared with the WT protein in proximity to the border of subunits. These findings collectively indicated that [2Fe-2S] cluster insertion is a key event in folding the dimerization domain of AOX1. The [2Fe-2S] cluster typically mediates electron transfer from Moco to FAD. Additionally, the monomer of AOX1 has been reported to be less saturated with iron and molybdenum than the dimer in WT and R802C (Hartmann et al., 2012). This result revealed the importance of the [2Fe-2S] cluster in dimer formation, although the stabilizing effect of the structure remains to be determined. Therefore, the reduced [2Fe-2S] cluster content in T755I may be responsible for dimer formation and reduced enzyme activity. However, we did not measure the saturation of the [2Fe-2S] cluster at SNPs. Therefore, the effect of the AOX1 cofactor on the complex formation of the variant is still unknown. Consequently, further studies are necessary to clarify the role of the [2Fe-2S] cluster and the dimerization mechanism.

Data regarding the allele frequencies of AOX1 obtained from genome databases revealed that the I598N, T755I, and H1297R mutants are commonly detected in East Asian populations. Among these, we found that I598N and H1297R tended to be associated with a reduction in the activity of AOX1, albeit this correlation was nonsignificant. Compared with the East Asian populations, N1135S, the most extensively investigated variant, is more frequently detected in African or European populations. However, although these differences in AOX1 variant frequencies may be linked to ethnic differences with respect to the pharmacokinetics and adverse effects of clinical drugs, at present, the involvement of AOX1 polymorphisms in drug treatment has yet to be reported in clinical studies of East Asian populations. Moreover, in addition to SNPs in AOX1, it has been reported that variants of

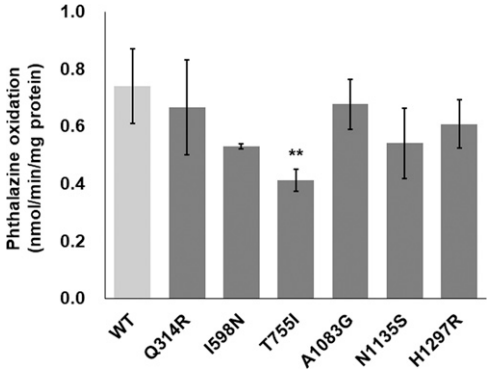

Fig. 4. Comparison of the oxidation of 1 μM phthalazine using S9 fractions from WT or variant AOX1 expressed in HEK293T cells. Assays were performed for 10 minutes at pH 7.4. $^{*}P < 0.05$ compared with the WT; Dunnett's test. Data represent the means plus or minus S.D. of three independent experiments.

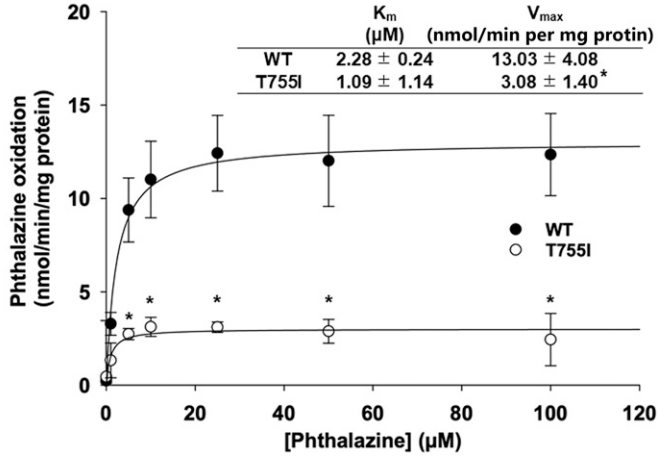

Fig. 5. Enzyme kinetic assay for the oxidation of phthalazine. Metabolism of 1–100 μM phthalazine to phthalazone was measured for 10 minutes at pH 7.4 using S9 fractions obtained from WT (filled circles) or T755I (open circles) AOX1 expressed in HEK293T cells. Plots were fitted to the Michaelis-Menten equation. $^{*}P < 0.05$ compared with the WT; unpaired Student's *t* test. Data represent the means plus or minus S.D. of three independent experiments.

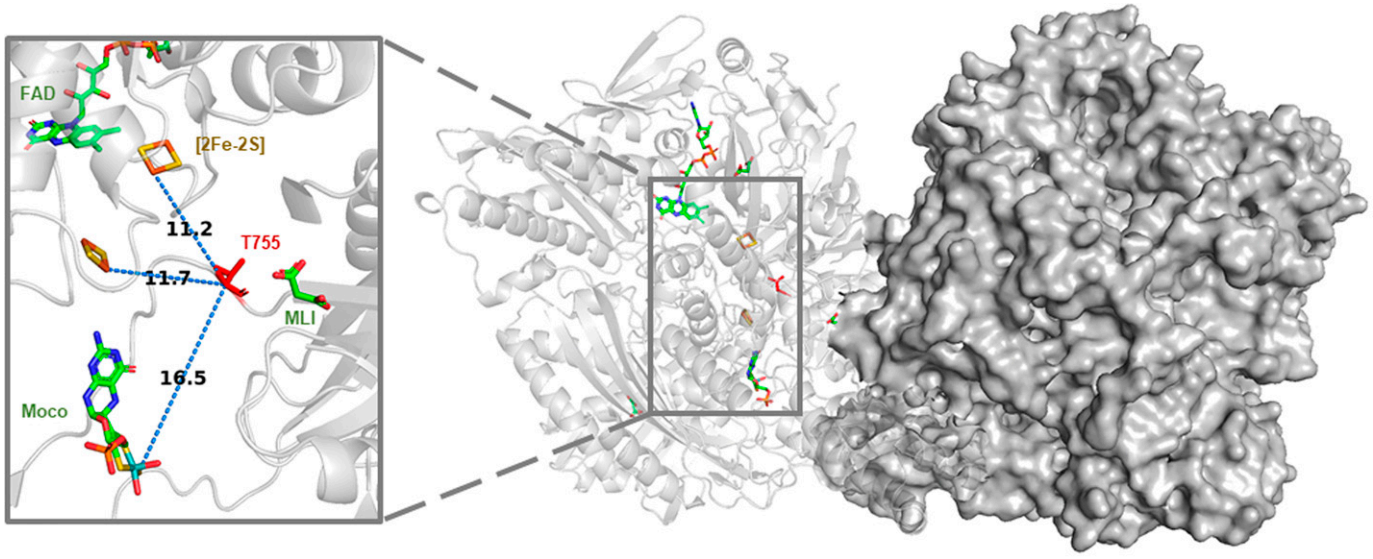

Fig. 6. Location of T755 in WT AOX1. The three-dimensional structure was obtained from the 4UHW Protein Data Bank. T755, FAD, Moco, the [2Fe-2S] cluster, and the malonate ion (MLI) are shown as stick representations. The AOX1 monomer of chain A is shown as a cartoon, and chain B as a surface representation. The distance from the mutated amino acids is denoted by dashed lines.

molybdenum cofactor sulfurase, which yields a cofactor of the molybdo-flavoenzyme, may influence the therapeutic effect of azathioprine (Smith et al., 2009; Kurzawski et al., 2012). Consequently, when assessing the clinical effects of SNPs associated with AOX activity, we should ideally take into consideration not only AOX1 mutants but also those of molybdenum cofactor sulfurase.

In conclusion, the T755I variant of the AOX1 protein was found to be associated with a reduction in enzyme activity linked to the suppression of dimer formation, although in the absence of any marked effect on protein expression. Given the broad substrate specificity of AOX1, it can be speculated that a reduction in enzyme activity induced by the T755I mutation—which appears to be particularly prevalent in East Asian populations—may have an appreciable influence on the therapeutic efficacy and/or toxicity of drugs in patients with this mutation. Further studies are thus warranted to confirm the clinical significance of the T755I variant and its influence on the treatment outcomes or toxicity of AOX1 substrate drugs.

Authorship Contributions

Participated in research design: Ueda, Narumi, Kobayashi.

Conducted experiments: Ueda, Narumi.

Performed data analysis: Ueda, Narumi.

Wrote or contributed to the writing of the manuscript: Ueda, Narumi, Furugen, Saito, Kobayashi.

References

Auton A, Brooks LD, Durbin RM, Garrison EP, Kang HM, Korbel JO, Marchini JL, McCarthy S, McVean GA, and Abecasis GR; 1000 Genomes Project Consortium (2015) A global reference for human genetic variation. *Nature* **526**:68–74.

Coelho C, Foti A, Hartmann T, Santos-Silva T, Leimkühler S, and Romão MJ (2015) Structural insights into xenobiotic and inhibitor binding to human aldehyde oxidase. *Nat Chem Biol* **11**:779–783.

Amano T, Fukami T, Ogiso T, Hirose D, Jones JP, Taniguchi T, and Nakajima M (2018) Identification of enzymes responsible for dantrolene metabolism in the human liver: A clue to uncover the cause of liver injury. *Biochem Pharmacol* **151**:69–78.

Coelho C, Muthukumaran J, Santos-Silva T, and João Romão M (2019) Systematic exploration of predicted destabilizing nonsynonymous single nucleotide polymorphisms (nsSNPs) of human aldehyde oxidase: A Bio-informatics study. *Pharmacol Res Perspect* **7**:e00538.

Demir E, Sütcüoğlu O, Demir B, Ünsal O, and Yazõcõ O (2022) A possible interaction between favipiravir and methotrexate: Drug-induced hepatotoxicity in a patient with osteosarcoma. *J Oncol Pharm Pract* **28**:445–448.

Foti A, Hartmann T, Coelho C, Santos-Silva T, Romão MJ, and Leimkühler S (2016) Optimization of the Expression of Human Aldehyde Oxidase for Investigations of Single-Nucleotide Polymorphisms. *Drug Metab Dispos* **44**:1277–1285.

Fu C, Di L, Han X, Soderstrom C, Snyder M, Troutman MD, Obach RS, and Zhang H (2013) Aldehyde oxidase 1 (AOX1) in human liver cytosols: quantitative characterization of AOX1 expression level and activity relationship. *Drug Metab Dispos* **41**:1797–1804.

Garattini E, Fratelli M, and Terao M (2008) Mammalian aldehyde oxidases: genetics, evolution and biochemistry. *Cell Mol Life Sci* **65**:1019–1048.

Garattini E, Mendel R, Romão MJ, Wright R, and Terao M (2003) Mammalian molybdo-flavoenzymes, an expanding family of proteins: structure, genetics, regulation, function and pathophysiology. *Biochem J* **372**:15–32.

Hartmann T, Terao M, Garattini E, Teutloff C, Alfaro JF, Jones JP, and Leimkühler S (2012) The impact of single nucleotide polymorphisms on human aldehyde oxidase. *Drug Metab Dispos* **40**:856–864.

Hutzler JM, Yang YS, Brown C, Heyward S, and Moeller T (2014) Aldehyde oxidase activity in donor-matched fresh and cryopreserved human hepatocytes and assessment of variability in 75 donors. *Drug Metab Dispos* **42**:1090–1097.

Itoh K, Maruyama H, Adachi M, Hoshino K, Watanabe N, and Tanaka Y (2007) Lack of formation of aldehyde oxidase dimer possibly due to 377G>A nucleotide substitution. *Drug Metab Dispos* **35**:1860–1864.

Karczewski KJ, Francioli LC, Tiao G, Cummings BB, Alföldi J, Wang Q, Collins RL, Laricchia KM, Ganna A, Birnbaum DP et al.; Genome Aggregation Database Consortium (2020) The mutational constraint spectrum quantified from variation in 141,456 humans. *Nature* **581**:434–443.

Kitamura S, Sugihara K, and Ohta S (2006) Drug-metabolizing ability of molybdenum hydroxylases. *Drug Metab Pharmacokinet* **21**:83–98.

Konishi K, Fukami T, Gotoh S, and Nakajima M (2017) Identification of enzymes responsible for nitrazepam metabolism and toxicity in human. *Biochem Pharmacol* **140**:150–160.

Kurzawski M, Dziewanowski K, Safranow K, and Drozdzik M (2012) Polymorphism of genes involved in purine metabolism (XDH, AOX1, MOCOS) in kidney transplant recipients receiving azathioprine. *Ther Drug Monit* **34**:266–274.

Morgan SL and Baggott JE (2019) The importance of inhibition of a catabolic pathway of methotrexate metabolism in its efficacy for rheumatoid arthritis. *Med Hypotheses* **122**:10–15.

Obach RS, Huynh P, Allen MC, and Beedham C (2004) Human liver aldehyde oxidase: inhibition by 239 drugs. *J Clin Pharmacol* **44**:7–19.

Panoutsopoulos GI and Beedham C (2004) Enzymatic oxidation of phthalazine with guinea pig liver aldehyde oxidase and liver slices: inhibition by isovanillin. *Acta Biochim Pol* **51**:943–951.

Schumann S, Saggu M, Möller N, Anker SD, Lendzian F, Hildebrandt P, and Leimkühler S (2008) The mechanism of assembly and cofactor insertion into Rhodobacter capsulatus xanthine dehydrogenase. *J Biol Chem* **283**:16602–16611.

Smith MA, Marinaki AM, Arenas M, Shobowale-Bakre M, Lewis CM, Ansari A, Duley J, and Sanderson JD (2009) Novel pharmacogenetic markers for treatment outcome in azathioprine-treated inflammatory bowel disease. *Aliment Pharmacol Ther* **30**:375–384.

Tai LA and Hwang KC (2004) Cooperative catalysis in the homodimer subunits of xanthine oxidase. *Biochemistry* **43**:4869–4876.

Tamura K, Stecher G, and Kumar S (2021) MEGA11: Molecular Evolutionary Genetics Analysis Version 11. *Mol Biol Evol* **38**:3022–3027.

Address correspondence to: Dr. Katsuya Narumi, Hokkaido University, Kita-12-jo, Nishi-6-chome, Kita-ku, 060-0812 Sapporo, Japan. E-mail: narumik@pharm.hokudai.ac.jp; or Dr. Masaki Kobayashi, Hokkaido University, Kita-12-jo, Nishi-6-chome, Kita-ku, 060-0812 Sapporo, Japan. E-mail: masaki@pharm.hokudai.ac.jp